Plastic Strength of Connection Elements

BO DOWSWELL

ABSTRACT

Many connection elements are modeled as rectangular members under various combinations of shear, flexural, torsional and axial loads. Strength design is now used for steel members and connections; therefore, the traditional method of combining loads using beam theory needs to be updated to comply with strength design philosophy. Due to the extensive research available on the plastic interaction of rectangular members, a review of existing equations forms the basis of this paper. In cases where existing research is unavailable, new derivations are provided. An interaction equation is developed for strength design of rectangular connection elements under any possible loading combination.

Keywords: connections, plastic design, rectangular elements.

INTRODUCTION

For design, connections are divided into elements and modeled as structural members with well-documented and predictable behavior. Many connection elements can be modeled as rectangular members under various combinations of shear, flexural, torsional and axial loads. Traditionally, loads have been combined using beam equations with a first-yield criterion; however, a plastic strength approach is more appropriate for connections designed to the AISC *Specification* (AISC, 2010), which is based on a strength design philosophy.

The purpose of this paper is to determine the strength of rectangular connection elements subjected to various loads acting simultaneously. An interaction equation is developed for strength design of rectangular connection elements under any possible loading combination. Due to the extensive research available on the plastic interaction of rectangular members, a review of existing equations forms the basis of this paper. In cases where existing research is unavailable, new derivations are provided.

Rectangular Connection Elements

Figure 1a shows a moment connection, where the flange plates are modeled as rectangular members under axial tension and compression loads. Although other loads—such as a portion of the beam shear—will transfer through the flange plates, inelastic material behavior will allow load redistribution in ductile connection elements. This redistribution of loads allows the flange plates to be designed based on the simplified assumption of axial load only.

Bo Dowswell, P.E., Ph.D., Principal, ARC International, LLC, Birmingham, AL. Email: bo@arcstructural.com

Paper No. 2013-21

Figure 1b shows a single-plate connection, which is subjected to a constant shear load and a maximum moment at the face of the column. In some cases, such as for drag strut connections, these connections must also carry a substantial axial load. Because the moment, shear and axial loads occur at the same location on the connection element, the load interaction must be accounted for. Although typically neglected in design, twisting deformations in tests by Moore and Owens (1992), Sherman and Ghorbanpoor (2002) and Goodrich (2005) have shown that torsional stresses are also present.

The bracket, gusset and hanger connections in Figures 1c through 1e are additional examples of rectangular connection elements subjected to strong-axis bending in addition to shear and/or axial loads. Figure 1f shows the prying action of a flange, which is a rectangular connection element in weak-axis bending. In this case, the effect of the shear force is usually small and is neglected in practice.

Von Mises Criterion

Several theories have been proposed to predict the behavior of materials under multiaxial states of stress. Von Mises' criterion is considered the most accurate for predicting the initiation of yield in ductile metals when loaded by various combinations of normal and shear stresses. For plane stress, von Mises' equation reduces to

$$\sigma_e = \sqrt{\sigma_x^2 + \sigma_z^2 - \sigma_x \sigma_z + 3\tau^2} \quad (1)$$

where

σ_e = effective stress, ksi
σ_x = normal stress in the x-direction, ksi
σ_z = normal stress in the z-direction, ksi
τ = shear stress, ksi

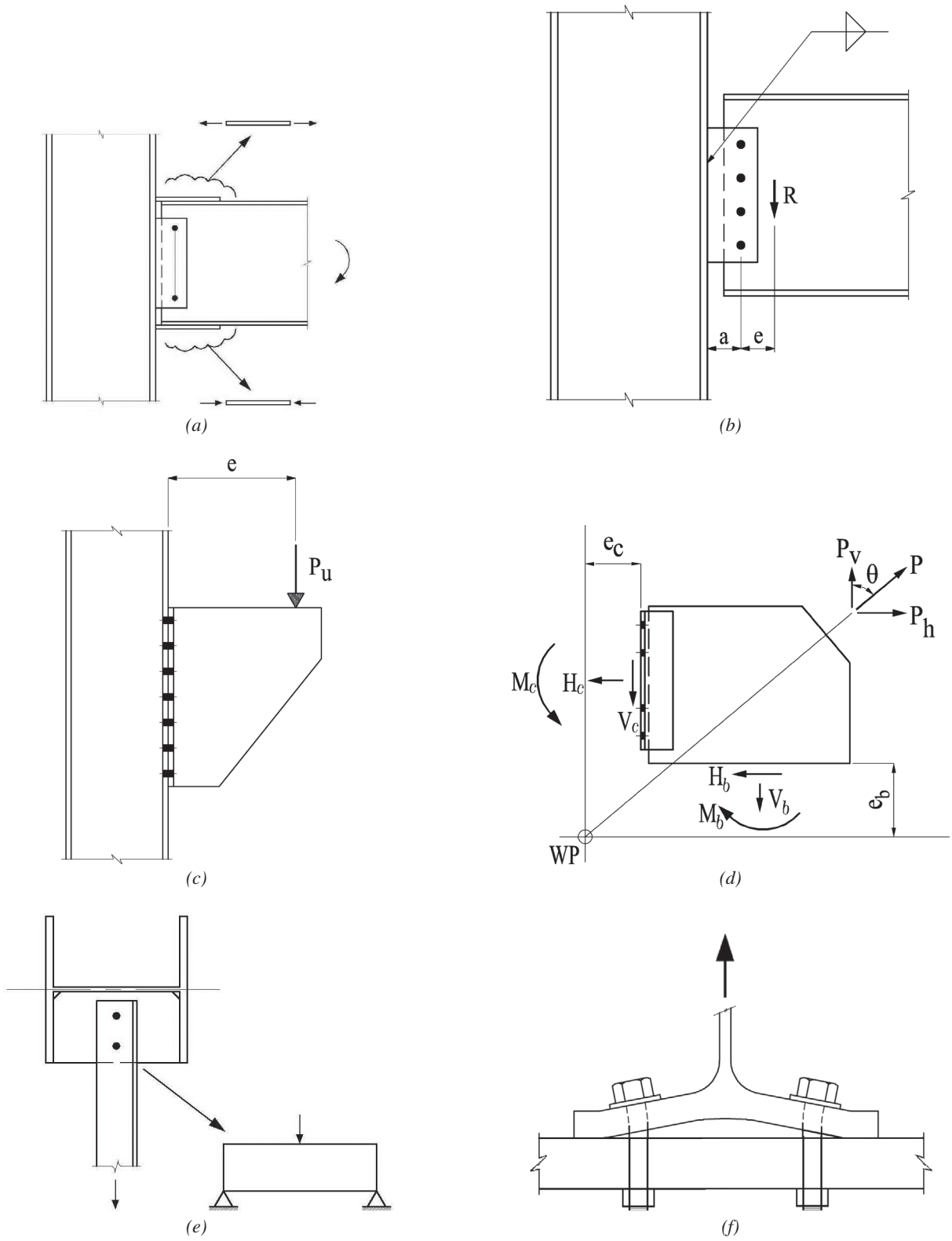

Fig. 1. Rectangular connection elements: (a) moment connection; (b) single-plate connection; (c) bracket; (d) gusset plate; (e) hanger plate; (f) prying at flange.

For elastic conditions, σ_e is limited to the tension yield strength of the steel, σ_y.

The Need for Plastic Interaction Equations

Historically, rectangular connection elements have been designed using beam theory. The normal and shear stresses are calculated with Equations 2 and 3, respectively:

$$\sigma = \frac{P}{A} \pm \frac{Mc}{I} \tag{2}$$

$$\tau = \frac{VQ}{It} \tag{3}$$

where

A = cross-sectional area, in.^{2}
M = bending moment, in.-kips
P = axial force, kips
Q = first moment of area, in.^{3}
V = shear force, kips
I = moment of inertia, in.^{4}
c = distance to outermost fiber, in.
t = thickness of the member, in.

Because the maximum normal and shear stresses occur at different locations on the cross-section, combining these stresses is not required.

To predict the true first yield load in a member, the residual stresses must be estimated. Connection elements are subjected to a wide variety of operations during manufacture, fabrication and erection. The edges have traditionally been rolled (bars and UM plates), saw-cut, sheared or thermally cut with an oxy-fuel torch. All of these operations produce different residual stress patterns. Adding to the complexity, the residual stress patterns produced by newer technologies—such as plasma cutting and water-jet cutting—are also different. Many of the cut edges are smoothed with an angle grinder, which can alter the residual stress pattern, causing a residual tension stress in most cases. A general assessment of residual stresses that accounts for all of these factors is impractical. However, because residual stresses have no effect on the plastic strength of an element, knowledge of the residual stresses are not required for strength design.

It is well known that beam theory is inaccurate at low span-to-depth ratios. Research by Karr (1956), Shawki and Hendry (1961) and Barry and Ainso (1983) generally agreed that beam theory is accurate only for simple beams with span-to-depth ratios of at least 1.5. Ahmed, Idris and Uddin (1996) showed that fixed-end beams require a span-to-depth ratio of at least 3 to get accurate results with beam theory. Tests on gusset plates by Wyss (1923), Rust (1938), Perna (1941), Sandel (1950), Whitmore (1952), Sheridan (1953), Irvan (1957), Hardin (1958), Lavis (1967) and Vasarhelyi (1971) showed that measured shear and normal stresses deviated significantly from the theoretical stresses calculated with beam equations. This was confirmed by the finite element models of Struik (1972) and White et al. (2013).

Beam theory leads to erroneous results for some plate geometries. In Figure 2a, a simple hanger connection is shown where, if $a = b$, the gusset plate is subjected to a uniform tension stress. Figure 2b shows a plot of the normalized strength versus the b/a ratio. The normalized strength is

$$\frac{P_n}{2atF_y} \tag{4}$$

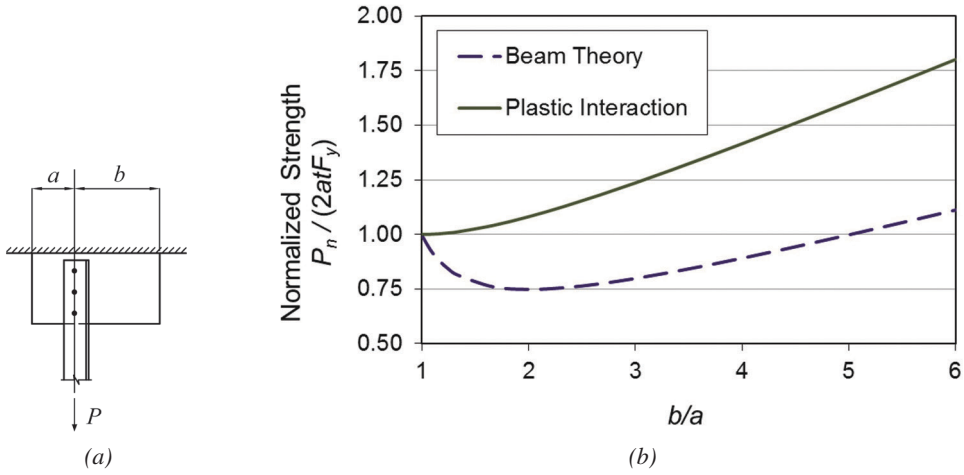

Fig. 2. Hanger connection with axial load and moment: (a) connection geometry; (b) normalized strength versus b/a ratio.

where

P_n = nominal axial strength, kips
a = plate dimension as shown in Figure 2a, in.
= half plate width for concentrically loaded case
F_y = specified minimum yield strength, ksi

If a remains constant and b increases, it is intuitive that that the strength of the gusset plate will increase; however, the dashed line in Figure 2b shows that beam theory predicts a decrease in strength in the range $1 < b/a < 5$. For the case where $b = 2a$, the plate is 50% wider than if $b = a$, but beam theory predicts only 75% of the strength. Plastic interaction, shown in Figure 2b by the solid line, conforms to the expected result—the strength increases as the plate width increases.

Strength design is now used for steel members and connections; therefore, the traditional method of combining loads using beam theory needs to be updated to comply with strength design philosophy. With difficulties in predicting the elastic stresses, the presence of discontinuities and uncertainty concerning residual stresses, plastic interaction equations are required to accurately predict the strength of connection elements.

BENDING

Due to a shape factor of 1.5, the benefit of using the plastic flexural strength of rectangular members is substantial. For this strength to be realized, the element must have sufficient rotational capacity to allow the stresses to redistribute without rupture or buckling. Schreiner (1935) and Jensen and Crispen (1938) tested cantilever plates in strong-axis bending, welded to a fixed support. They determined that the plates, which had maximum depth-to-thickness ratios of 10, can reach their plastic bending strength. More recently, tests on single-plate connections by Patrick, Thomas and Bennetts (1986) and Metzger (2006) revealed that the plastic moment capacity of the plate can be used in design.

Assuming no residual stresses, the flexural stiffness is linear up to the yield moment, M_y, and then the curve becomes nonlinear up to a maximum value of $M = M_p = 1.5M_y$, as shown in Figure 3. The inelastic part of the curve, defined by Equation 5, was derived by Nadai (1950) using linear elastic–perfectly plastic material behavior:

$$\frac{M}{M_p} = 1 - \frac{1}{3}\left(\frac{\theta_y}{\theta}\right)^2 \tag{5}$$

where

M_p = plastic bending moment, in.-kips
θ = flexural rotation
θ_y = yield rotation

To develop 96% of the plastic strength, a rotation of three times the yield rotation is required. At four times the yield rotation $M = 0.98M_p$.

Based on 14 splice plates tested in bending, Mohr and Murray (2008) determined that the flexural strength can be calculated based on the gross plastic modulus if deformation of the connection plates is not a consideration. The tests showed that the location of the initial nonlinear part of the moment-rotation curve can be accurately predicted using the first yield moment

$$M_y = \sigma_y S \tag{6}$$

where

S = gross section modulus, in.^{3}
σ_y = tension yield stress, ksi

The nominal plastic moment about the strong and weak axes are calculated with Equations 7a and 7b, respectively:

$$M_{px} = F_y Z_x \tag{7a}$$

$$M_{pz} = F_y Z_z \tag{7b}$$

The plastic moduli about the strong and weak axes are given by Equations 8a and 8b, respectively:

$$Z_x = \frac{td^2}{4} \tag{8a}$$

$$Z_z = \frac{dt^2}{4} \tag{8b}$$

where

d = depth of the member, in.

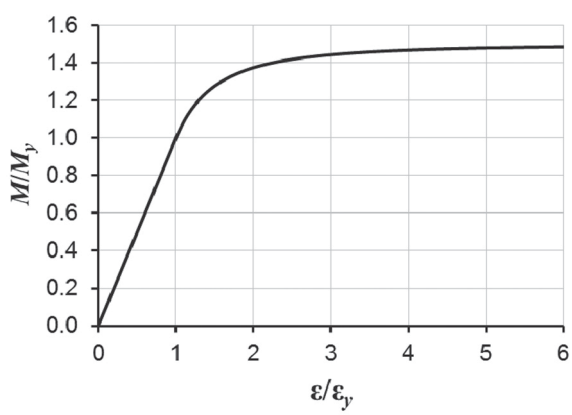

Fig. 3. Normalized moment versus normalized angle of rotation.

AXIAL

It is generally accepted that the compression yield strength is the same as the tension yield strength for ductile steels. This was verified by Seely and Putnam (1919), who showed that the compression yield strengths for mild and medium steels are about 5% greater than the tension yield strengths. The nominal axial yield force for tension or compression loads is

$$P_y = F_y A \tag{9}$$

SHEAR

Using the von Mises criterion, the shear yield stress is

$$\begin{aligned}\tau_y &= \frac{\sigma_y}{\sqrt{3}} \\ &= 0.577\sigma_y\end{aligned} \tag{10}$$

Seely and Putnam (1919) tested 21 solid circular specimens in torsion to determine the tension yield-to-shear yield ratios. The specimens, between ½ in. and ¾ in. in diameter, showed that the shear yield strength for mild and medium steels varied from 0.628 to 0.738 times the tension yield strengths. Therefore, the von Mises criterion appears to be conservative.

Based on three chevron gusset plate tests, Astaneh (1992) recommended that the plastic stress distribution be used to calculate the shear strength of gusset plates. Tests on full-scale truss bridge gusset plates by Ocel (2013) and finite element models by White et al. (2013) confirmed Astaneh's recommendation. The shear strength, based on a plastic stress distribution, is

$$V_p = \tau_y A \tag{11}$$

AISC *Specification* (AISC, 2010) Section J4.2 rounds the 0.577 factor up to 0.60, which results in a nominal shear force of

$$V_p = 0.60 F_y A \tag{12}$$

TORSION

The elastic solution for a uniform member with constant torque was solved by Saint Venant. Saint Venant torsion, also known as *uniform torsion*, assumes the applied torque is resisted by shear stresses distributed over the cross-section. This section addresses uniform torsion only and neglects the effects of warping and the Wagner effect, which causes second-order axial stresses resulting in an increased torsional stiffness (Gregory, 1960).

The rate of twist of an elastic member under uniform torsion is (Cook and Young, 1985)

$$\begin{aligned}\beta &= \frac{d\theta}{dx} \\ &= \frac{T}{GJ}\end{aligned} \tag{13}$$

For uniform members with constant torque along the length of the member, the angle of twist is the rate of twist times the member length.

$$\begin{aligned}\theta &= \beta L \\ &= \frac{TL}{GJ}\end{aligned} \tag{14}$$

where

G = shear modulus of elasticity = 11,200 ksi
J = torsional constant, in.^{4}
L = length of the member, in.
T = torsional moment, in.-kips
x = distance along the length of the member, in.
θ = angle of twist

Generally, the torsional constant for a rectangular member is

$$J = \alpha d t^3 \tag{15}$$

According to Seaburg and Carter (1997), $\alpha = ⅓ - 0.2t/d$ for $d/t < 10$ and $\alpha = ⅓$ for $d/t \geq 10$. The results using these simple equations are almost identical to the slightly more complicated equations developed by Balaz and Kolekova (2002). The torsional first yield moment is

$$T_y = \frac{\tau_y J}{t} \tag{16}$$

For $d/t \geq 10$, which satisfies the geometry for most connection elements,

$$T_y = \frac{\tau_y d t^2}{3} \tag{17}$$

When loaded beyond the yield point, the behavior of rectangular members in uniform torsion is similar to inelastic flexural behavior. Smith and Sidebottom (1965) derived the mathematical description of the inelastic part of the torsion-twist curve:

$$\frac{T}{T_y} = \frac{3}{2}(1-\eta) - \frac{1-\eta}{2\left(\theta/\theta_y\right)^2} + \eta\left(\frac{\theta}{\theta_y}\right) \tag{18}$$

where

η = strain hardening modulus for pure shear

θ_y = yield rotation

The accuracy of Equation 18 has been verified by the inelastic finite element models of Shunsuke and Kajita (1982) and May and Al-Shaarbaf (1989). The yield rotation can be determined by substituting Equation 16 into Equation 14:

$$\theta_y = \frac{\tau_y L}{Gt} \tag{19}$$

Due to the torsional flexibility of rectangular members, it is unlikely that they will strain beyond the yield plateau of mild steel. Therefore, $\eta = 0$ in the range of serviceable rotations, which gives the equation for linear elastic–perfectly plastic material behavior:

$$\frac{T}{T_y} = 1.5 - 0.5\left(\frac{\theta_y}{\theta}\right)^2 \tag{20}$$

The torsional stiffness is linear up to the yield moment, T_y, and then the curve becomes nonlinear up to a maximum value of $T = T_p = 1.5T_y$, as shown in Figure 4. Substituting $T_p = 1.5T_y$ into Equation 20 results in Equation 21, which was derived independently by Billinghurst et al. (1992):

$$\frac{T}{T_p} = 1 - \frac{1}{3}\left(\frac{\theta_y}{\theta}\right)^2 \tag{21}$$

where

T_p = plastic torsional moment, in.-kips

Equation 21 has the identical form of Equation 5, which was derived for flexural rotation. To develop 96% of the plastic strength, a rotation of three times the yield rotation is required. At four times the yield rotation $T = 0.98T_p$.

The plastic torsion strength can also be derived using the stress function. For any stress condition, the torsion strength is twice the volume under the stress function, ϕ (Smith and Sidebottom, 1965). Therefore, the plastic strength can be determined with Equation 22:

$$T_p = 2\int\int \phi \, dx dz \tag{22}$$

where

x, z = cross-sectional coordinates

The absolute value of the slope of ϕ everywhere on the cross-section is τ_y for fully plastic conditions. At the boundaries of the cross-section, ϕ must be zero, and the value of ϕ at any point on the cross-section is τ_y times the perpendicular distance to the boundary. This stress condition, known as the sand heap analogy, is illustrated in Figure 5.

For rectangular members with high aspect (d/t) ratios, the boundary effects parallel to the longest cross-sectional dimension can be neglected. In this case, the stress function is two-dimensional and the plastic strength is

$$\begin{aligned} T_p &= 2d\tau_y \int_{-t/2}^{t/2} x \, dx \\ &= 4d\tau_y \int_{-t/2}^{0} x \, dx \\ &= \frac{\tau_y d t^2}{2} \end{aligned} \tag{23}$$

By comparing Equation 17 to Equation 23, it can be seen that $T_p = 1.5T_y$. The nominal torsion strength is

$$T_p = 0.3F_y dt^2 \tag{24}$$

INTERACTION

A review of the existing research indicated that plastic interaction equations for several loading combinations have been available for decades. This section of the paper documents the available research, compares the different interaction equations, develops new equations where existing research

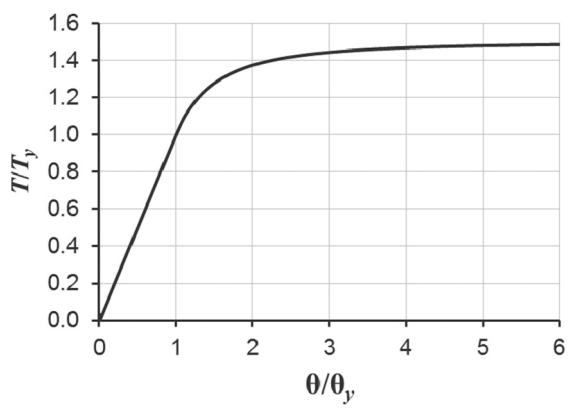

Fig. 4. Normalized torsion versus normalized angle of twist.

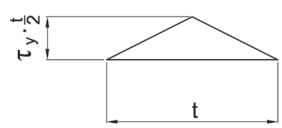

Fig. 5. Stress distribution for plastic torsional strength.

is unavailable and compares the equations to test data where available.

The derivations are based on assumed stress distributions, which complies with the lower-bound theorem of limit analysis. According to the lower-bound theorem, a load calculated with an assumed distribution that satisfies equilibrium, with stresses nowhere exceeding the yield stress, will be less than or equal to the true limit load. Where more than one solution is available, the solution that gives the highest strength is closest to the true strength. All interaction equations discussed in this paper assume perfectly plastic material behavior under plane stress conditions.

Moment-Axial Interaction

Because axial and flexural loads both cause normal stresses in the member, engineers may simply replace the section modulus with the plastic modulus in the beam equation, which results in a linear interaction. This is a conservative assumption because the stresses can be combined using the lower-bound theorem, which allows the axial stresses to be placed at a location that is least detrimental to the flexural strength.

Freudenthal (1950) derived the plastic interaction equation for combined axial and flexural loads. Also see Seely and Smith (1952), Vrouwenvelder (2003), Chen and Han (2007) and Galambos and Surovek (2008) for similar approaches to the derivation with identical results. The derivation is based on the assumed stress blocks in Figure 6, which locates the resistance to axial load at the center of the cross-section because the outer stress blocks are most efficient for flexural resistance.

The reduced axial strength in the presence of an applied moment is defined by the area of the shaded part of Figure 6:

$$P = ht\sigma_y \tag{25}$$

where

h = depth of the central region of the cross-section resisting the axial force, in.

The reduced flexural strength in the presence of an applied axial load is defined by the nonshaded part of Figure 6:

$$M = \frac{td^2}{4}\sigma_y - \frac{th^2}{4}\sigma_y \tag{26}$$

The axial strength ratio is

$$\frac{P}{P_y} = \frac{ht\sigma_y}{dt\sigma_y} = \frac{h}{d} \tag{27}$$

The flexural strength ratio is

$$\frac{M}{M_p} = \frac{\frac{td^2}{4}\sigma_y - \frac{th^2}{4}\sigma_y}{\frac{td^2}{4}\sigma_y} = 1 - \left(\frac{h}{d}\right)^2 \tag{28}$$

Combining Equations 27 and 28 results in Equation 29:

$$\frac{M}{M_p} + \left(\frac{P}{P_y}\right)^2 = 1.0 \tag{29}$$

Equation 29 is plotted in Figure 7 along with the interaction according to beam theory. For comparison, the interaction

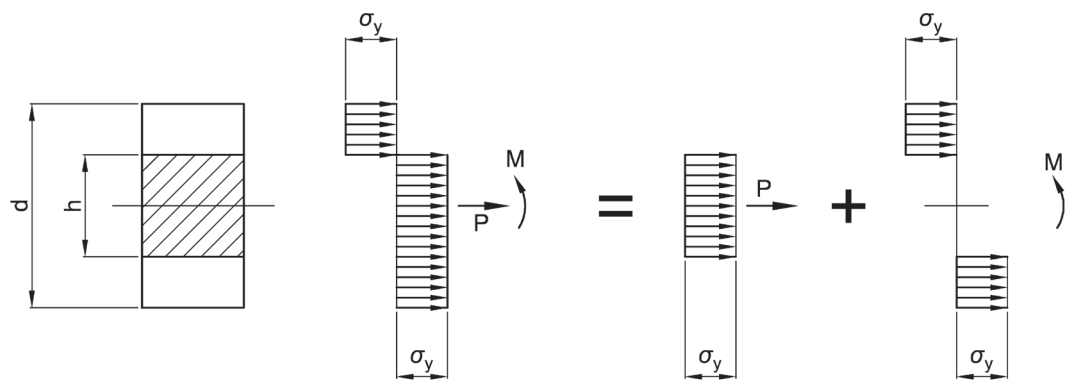

Fig. 6. Stress blocks for moment-axial interaction.

curves of AISC *Specification* Sections H1 and H2 are also plotted in the figure.

The plastic interaction equations were verified by the experiments of Sidebottom and Clark (1958), who tested nine identical, mild steel rectangular members. The specimens had a yield stress of 30 ksi and a modulus of elasticity of 30,000 ksi. The cross-sectional dimensions were 0.900 in. × 1.15 in. An axial compression load was applied with an eccentricity of 0.345 in. causing strong-axis moment. Using Equation 29, the test-to-predicted ratio ranged from 0.926 to 1.12, with an average of 0.990.

Moment-Shear Interaction

Because the maximum shear and normal stresses act at the same location on the cross-section, the flexural strength can be reduced in the presence of shear loading. In contrast to moment-axial interaction, which has a unique solution, several solutions are available for moment-shear interaction. Derivations and assumed stress distributions are provided only where they relate to later parts of this paper.

An elliptical interaction equation can be derived, based on von Mises' criterion with a constant shear stress assumed over the cross-section. For normal stress in one direction combined with shear, von Mises' criterion reduces to

$$\sigma_y = \sqrt{\sigma^2 + 3\tau^2} \tag{30}$$

where

σ = normal stress, ksi

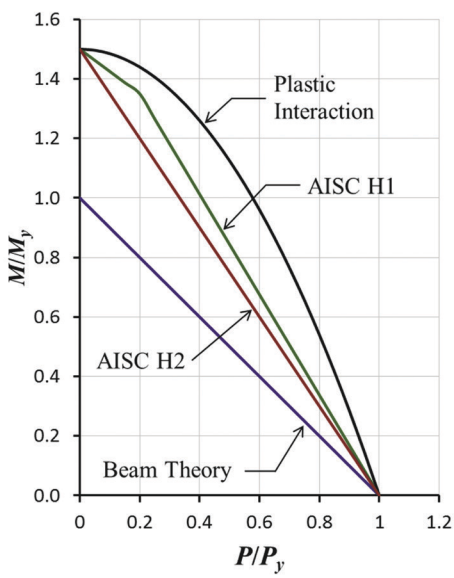

Fig. 7. Interaction of flexural and axial loads.

The moment and shear loads acting on the cross-section are given by Equations 31 and 32, respectively:

$$M = \frac{\sigma t d^2}{4} \tag{31}$$

$$V = \tau t d \tag{32}$$

The plastic flexural strength with no shear is

$$M_p = \sigma_y \frac{t d^2}{4} \tag{33}$$

The plastic shear strength with no moment is

$$V_p = \frac{\sigma_y}{\sqrt{3}} t d \tag{34}$$

Solving Equations 31 and 32 for σ and τ, respectively, substituting into Equation 30 and combining with Equations 33 and 34 results in Equation 35:

$$\left(\frac{M}{M}\right)^2 + \left(\frac{V}{V}\right)^2 = 1.0 \tag{35}$$

Paltchevskiy (1948) (see translation in Mrazik, Skaloud and Tochacek, 1987) assumed rectangular stress blocks for shear and flexural stresses as shown in Figure 8a. Based on this, the flexural strength is

$$M = M_p \left[1 - \left(\frac{h}{d}\right)^2\right] \tag{36}$$

where

h = depth of the central region of the cross-section resisting the shear force, in.

The shear strength is

$$V = V_p \left(\frac{h}{d}\right) \tag{37}$$

Solving Equation 37 for h/d and substituting into Equation 36 results in Equation 38:

$$\frac{M}{M_p} + \left(\frac{V}{V_p}\right)^2 = 1.0 \tag{38}$$

By considering equilibrium of the shear and flexural loads in the plastic zone of a rectangular beam, Horne (1951) derived Equation 39, which is valid for $V/V_p \le 0.792$. The shear yield strength was based on the Tresca criterion, which results in a shear yield stress of $\sigma_y/2$:

$$\frac{M}{M_p} + 0.444\left(\frac{V}{V_p}\right)^2 = 1.0 \tag{39}$$

Substituting a shear yield stress of $0.6\alpha_y$ changes the constant to 0.592 and the range of validity to $V/V_p \le 0.686$:

$$\frac{M}{M_p} + 0.592\left(\frac{V}{V_p}\right)^2 = 1.0 \tag{40}$$

Broude (1953) (see translation in Mrazik et al., 1987) developed a solution, based on the differential equations of equilibrium, that he solved for several discrete values. He determined a close curve fit to the discrete values, which is almost identical to the elliptical equation derived from the von Mises' criterion:

$$\left(\frac{M}{M_p}\right)^2 + \left(\frac{V}{V_p}\right)^2 - 0.0074\left(\frac{M}{M_p}\right)^2\left(\frac{V}{V_p}\right)^2 = 1.0 \tag{41}$$

Based on equilibrium of rectangular and triangular blocks for flexural stresses and a parabolic block for shear stresses, Neal (1963) (also see Chakrabarty, 2006) derived Equation 44. The assumed cross-sectional stresses are shown in Figure 8b. Based on equilibrium of the stress blocks, the flexural and shear strengths are given by Equations 42 and 43, respectively:

$$M = \frac{\sigma_y t}{4}\left(d^2 - \frac{h^2}{3}\right) \tag{42}$$

$$V = \frac{2}{3}\tau_y t h \tag{43}$$

Solving Equation 43 for y, substituting into Equation 42 and combining with Equations 33 and 34 results in Equation 44:

$$\frac{M}{M_p} + \frac{3}{4}\left(\frac{V}{V_p}\right)^2 = 1.0 \tag{44}$$

Because $h \le d$, Equation 44 is valid for the range $V/V_p \le 2/3$.

Drucker (1956) derived upper- and lower-bound solutions based on limit analysis theorems. Equation 45 was proposed as an approximation that "nearly coincides with a lower bound and is not too far from possible upper bounds":

$$\frac{M}{M_p} + \left(\frac{V}{V_p}\right)^4 = 1.0 \tag{45}$$

Johnson, Chitkara and Ranshi (1974) derived the plastic collapse strength using slip line fields. Their derivation was based on plane stress conditions using the von Mises yield criterion. Due to the complicated nature of the solution, it cannot be expressed as an interaction equation. Figure 9 shows the available solutions for moment-shear interaction. Because the curve defined by the slip line solution of Johnson et al. (1974) is the least conservative, it is closest to the true solution. Observation of the interaction equations reveals that the elliptical interaction defined by Equation 35 is more accurate at low values of M/M_p and Equation 45, developed by Drucker (1956), is more accurate at high values of M/M_p. Equations 35 and 45 are equal at $M/M_p = 0.618$ and $V/V_p = 0.786$. The solid data points are from tests on full-size gusset plates by Ocel (2013) and the hollow data points are from inelastic finite element models by White et al. (2013).

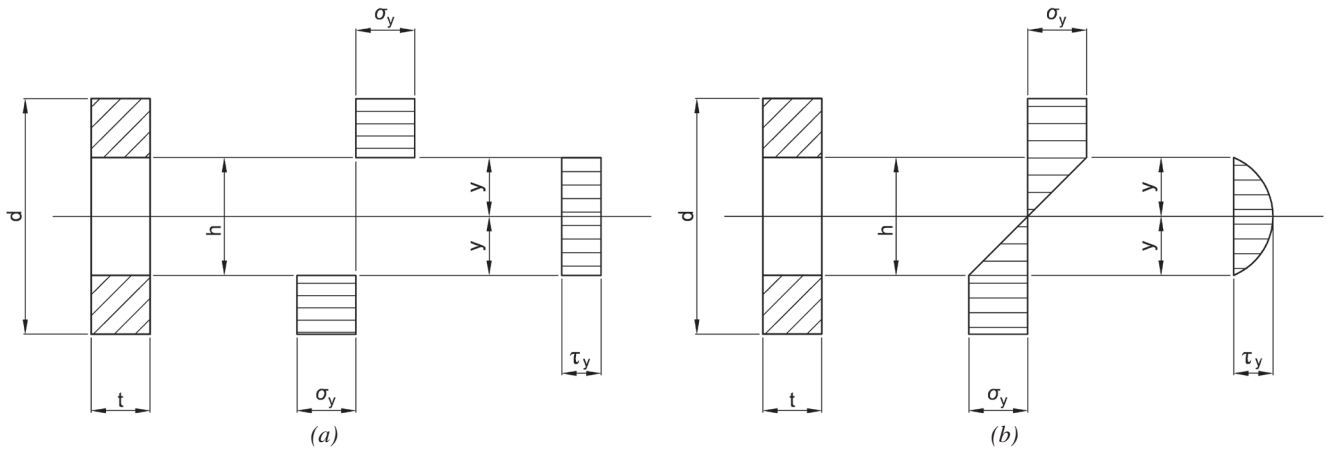

Fig. 8. Assumed stress blocks for moment-shear interaction: (a) Paltchevskiy (1948); (b) Neal (1963).

Moment-Shear-Axial Interaction

Neal (1961) derived upper- and lower-bound solutions for rectangular beams subjected to combined moment, shear and axial loads based on limit analysis theorems. Equation 46 was proposed as a "good approximation to the lower-bound interaction relation." He noted that the equation is exact for $V/V_p = 0$ and the discrepancy from the lower-bound solution never exceeds 5% for the full range of values:

$$\frac{M}{M_p}+\left(\frac{P}{P_y}\right)^2+\frac{\left(\frac{V}{V_p}\right)^4}{1-\left(\frac{P}{P_y}\right)^2}=1.0 \qquad (46)$$

Astaneh (1998) summarized the previous research and relevant code provisions for the seismic design of gusset plates. He removed second-order interaction on the shear term of Equation 46 and recommended Equation 47 for design:

$$\frac{M}{M_p}+\left(\frac{P}{P_y}\right)^2+\left(\frac{V}{V_p}\right)^4\le 1.0 \qquad (47)$$

Biaxial Bending

Using the lower-bound theorem of limit analysis, Harrison (1963) derived Equations 48a and b, which define a two-part interaction curve for biaxial bending.

When $M_x/M_{px} \ge 2/3$ and $M_z/M_{pz} < 2/3$,

$$\frac{M_x}{M_{px}}+\frac{3}{4}\left(\frac{M_z}{M_{pz}}\right)^2=1.0 \qquad (48a)$$

When $M_x/M_{px} < 2/3$ and $M_z/M_{pz} \ge 2/3$,

$$\frac{3}{4}\left(\frac{M_x}{M_{px}}\right)^2+\frac{M_z}{M_{pz}}=1.0 \qquad (48b)$$

where

M_{px} = plastic bending moment about the x-axis, in.-kips
M_{pz} = plastic bending moment about the z-axis, in.-kips
M_x = bending moment about the x-axis, in.-kips
M_z = bending moment about the z-axis, in.-kips

Harrison (1963) tested six mild steel rectangular members in biaxial bending. The cross-sectional dimensions were 0.300 in. × 0.500 in., and the yield strength was 36.6 ksi. The

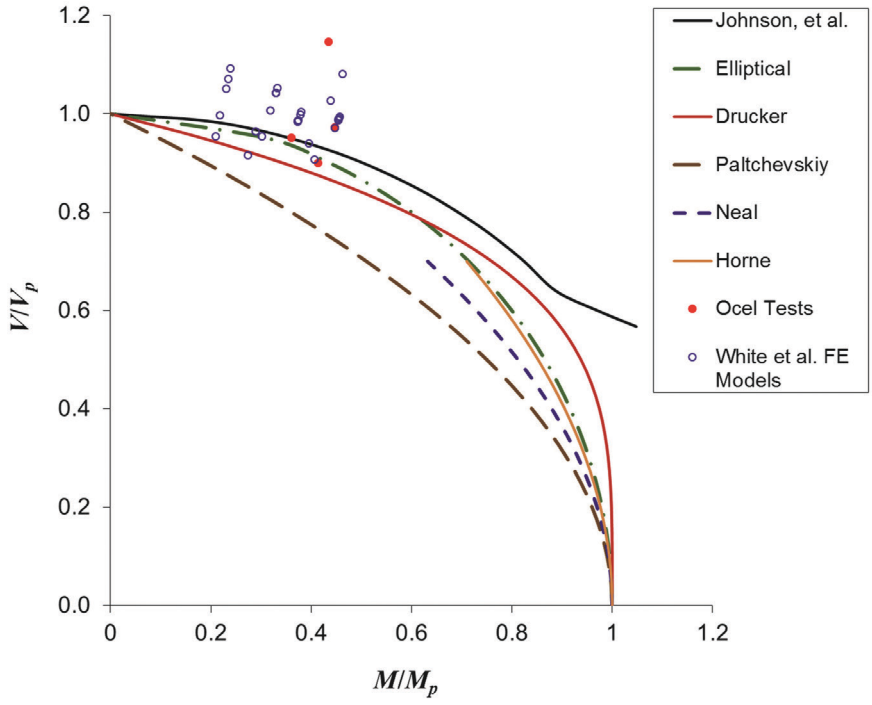

Fig. 9. Moment-shear interaction curves.

span was 18 in. with concentrated loads at ⅓ points, loading each principal axis. The ends were fixed against rotation in both directions. The interaction curve is in good agreement with the experimental results, with the greatest discrepancy being 4%. Figure 10 shows the experimental results plotted with the interaction curve defined by Equations 48a and b.

Axial Load Combined with Biaxial Bending

Santathadaporn and Chen (1970) (also see Chen and Atsuta, 1977) extended Equations 48a and b to include the effect of axial load. They presented the solution as a three-part interaction curve, defined by Equations 49a, b and c:

When $M_x/M_{px} \geq (⅔)(1 - P/P_y)$ and $M_z/M_{pz} < (⅔)(1 - P/P_y)$

$$\left(\frac{P}{P_y}\right)^2 + \frac{M_x}{M_{px}} + \frac{3}{4}\left(\frac{M_z}{M_{pz}}\right)^2 = 1.0 \qquad (49a)$$

When $M_x/M_{px} < (⅔)(1 - P/P_y)$ and $M_z/M_{pz} \geq (⅔)(1 - P/P_y)$

$$\left(\frac{P}{P_y}\right)^2 + \frac{3}{4}\left(\frac{M_x}{M_{px}}\right)^2 + \frac{M_z}{M_{pz}} = 1.0 \qquad (49b)$$

When $M_x/M_{px} \geq (⅔)(1 - P/P_y)$ and $M_z/M_{pz} \geq (⅔)(1 - P/P_y)$

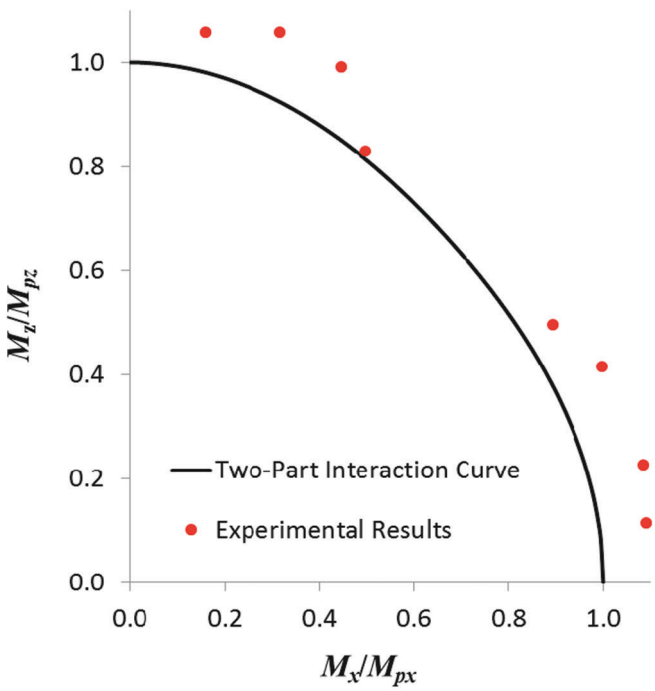

Fig. 10. Interaction curve for biaxial bending.

$$\left(\frac{P}{P_y}\right)^2 + \frac{9}{4}\left[1 - \frac{M_x}{2\left(1 - P/P_y\right)}\right]\left[1 - \frac{M_z}{2\left(1 - P/P_y\right)}\right] = 1.0 \qquad (49c)$$

Because these equations are cumbersome for design use, a single interaction equation can be developed as a best fit to the three-part curve. The continuous interaction curve developed by Duan and Chen (1989) for wide flange members is

$$\left(\frac{P}{P_y}\right)^2 + \left[\left(\frac{M_x}{M_{px}}\right)^\alpha + \left(\frac{M_z}{M_{pz}}\right)^\alpha\right]^{1/\alpha} = 1.0 \qquad (50)$$

Because the exponent, α, is not necessarily accurate for rectangular members, a new equation was developed by curve fitting the three-part curve. A numerical value of α was determined for each increment of P/P_y, which gave the best fit for that value of P/P_y. Equation 51 was determined by curve fitting all values of α:

$$\alpha = 1.7\left[1 - \frac{1}{4}\left(\frac{P}{P_y}\right) + \left(\frac{P}{P_y}\right)^2\right] \qquad (51)$$

The family of curves defined by Equations 50 and 51 are shown in Figure 11a. To simplify the equations, it may be beneficial to use a constant value of α. Figure 11b shows the family of curves defined by Equation 50 with α = 1.7. This solution appears to be adequate for design use, with the greatest discrepancies being conservative, at high P/P_y ratios.

Torsion-Shear Interaction

The interaction between torsion and shear loads is analogous to moment-axial interaction. The stresses in the central region of the cross-section are assigned to resist the shear force, and the torsional moment is resisted by the areas on the cross-section farthest from the shear center. The reduced shear strength in the presence of an applied torsional moment is defined by the area of the shaded part of Figure 12a:

$$V = bd\tau_y \qquad (52)$$

where

b = width of the central region of the cross-section resisting the shear force, in.

The reduced torsional strength in the presence of an applied shear load is defined by the nonshaded part of Figure 12a. From the diagram in Figure 12b,

$$T = 2\int\int \phi \, dx dz \tag{53}$$
$$= 4d\tau_y \int_{-t/2}^{-b/2} x \, dx$$
$$= \frac{\tau_y d}{2}\left(t^2 - b^2\right)$$

The shear strength ratio is

$$\frac{V}{V_p} = \frac{bd\tau_y}{td\tau_y} \tag{54}$$
$$= \frac{b}{t}$$

The torsional strength ratio is

$$\frac{T}{T_p} = \frac{\frac{\tau_y d}{2}\left(t^2 - b^2\right)}{\frac{\tau_y d t^2}{2}} \tag{55}$$
$$= 1 - \left(\frac{b}{t}\right)^2$$

Combining Equations 54 and 55 results in Equation 56.

$$\frac{T}{T_p} + \left(\frac{V}{V_p}\right)^2 = 1 \tag{56}$$

Equation 56 is plotted in Figure 13 along with the interaction according to elastic theory.

Moment-Axial-Torsion Interaction

Hill and Siebel (1953) (also see Chakrabarty, 2006) derived a lower-bound approximation for the interaction of axial, flexure and torsional loads:

$$\left(\frac{P}{P_y}\right)^2 + \left(\frac{T}{T_p}\right)^2 + \frac{M}{M_p}\sqrt{1 - \left(\frac{T}{T_p}\right)^2} = 1.0 \tag{57}$$

Calladine (1969) (also see Mrazik et al., 1987) recommended the following lower-bound interaction equations for use with all cross-sectional shapes. Calladine (1969) noted that with information on the cross-sectional shape, the equations could be refined and become less conservative:

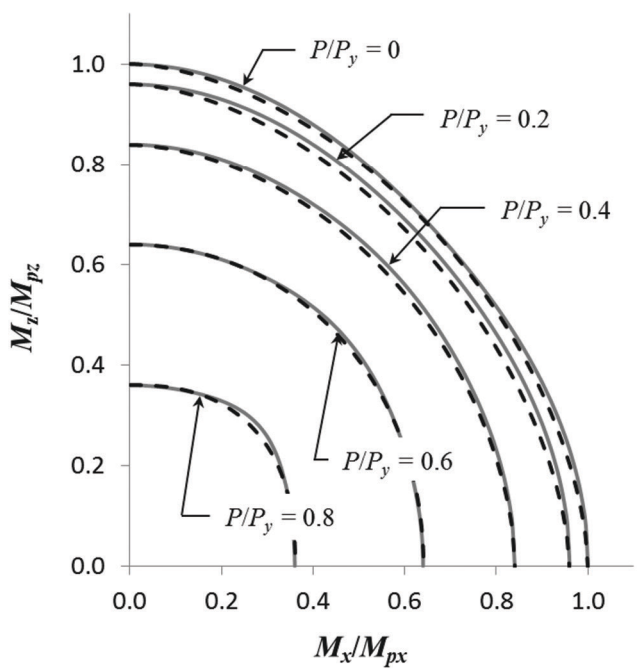

Solid lines defined by Equations 1
Dashed lines defined by Equations 49 and 50
(a)

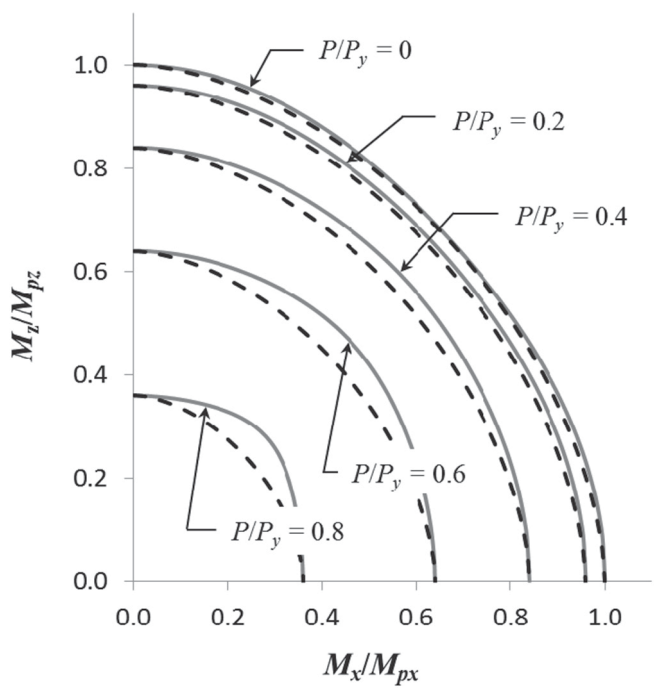

Solid lines defined by Equations 1
Dashed defined by Equation 49 with $\alpha = 1.7$
(b)

Fig. 11. Interaction curves for axial load and biaxial bending: (a) variable α; (b) constant α.

$$\left(\frac{T}{T_p}\right)^2+\left(\frac{P}{P_y}\right)^2=1.0 \tag{58}$$

$$\left(\frac{T}{T_p}\right)^2+\left(\frac{M}{M_p}\right)^2=1.0 \tag{59}$$

Equation 58 is equal to Equation 57 when $M = 0$, and Equation 59 is equal to Equation 57 when $P = 0$. Steele (1954) used the finite difference method to verify the accuracy of Equation 59. The equation was shown to give accurate lower-bound estimates of the interaction. Gill and Boucher (1964) tested 18 square and rectangular specimens in combined bending and torsion. The specimens were ⅝-in. × ⅝-in. and ⅜-in. × ⅝-in. cross-sections with a 12¾-in. span. The results are shown in Figure 14 along with Equation 59, which is clearly a lower bound to the test data.

Morris and Fenves (1969) derived a lower-bound solution for rectangular members under axial load, biaxial bending and torsion. The von Mises yield criterion was used to show that the reduced effective yield strength is

$$F_y'=\rho F_y \tag{60}$$

The yield strength reduction factor is

$$\rho=\sqrt{1-\left(\frac{T}{T_p}\right)^2} \tag{61}$$

As a general rule, interaction equations can be developed by multiplying any resisting load that produces a normal stress on the cross-section by ρ. For moment-axial-torsion interaction, this gives

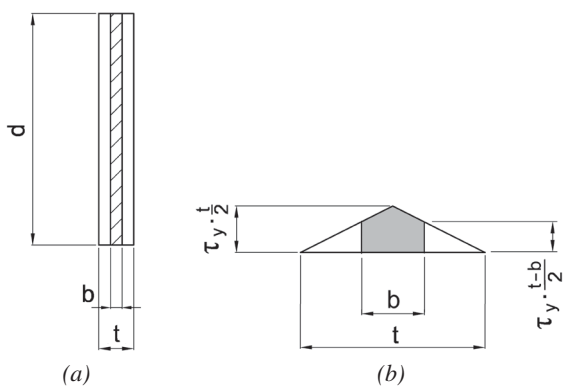

Fig. 12. Torsion-shear interaction: (a) cross-section; (b) torsion diagram.

$$\frac{\left(P/P_y\right)^2}{1-\left(T/T_p\right)^2}+\frac{M/M_p}{\sqrt{1-\left(T/T_p\right)^2}}=1.0 \tag{62}$$

If each side of the equation is multiplied by $1 - (T/T_p)^2$, it can be seen that Equation 62 is identical to Equation 57; therefore, the equations by Hill and Siebel (1952), Calladine (1969) and Morris and Fenves (1969) give identical results. Using the theory of Morris and Fenves, the interaction equation can be expanded to cover biaxial moments:

$$\left(\frac{P}{P_y}\right)^2+\left(\frac{T}{T_p}\right)^2+\left[\left(\frac{M_x}{M_{px}}\right)^\alpha+\left(\frac{M_z}{M_{pz}}\right)^\alpha\right]^{1/\alpha}\sqrt{1-\left(\frac{T}{T_p}\right)^2}=1.0 \tag{63}$$

DESIGN

To develop a single interaction equation that accounts for all loading possibilities, Equation 63 can be combined with Equation 45. This will account for all load interactions except torsion-shear. The reduction in shear strength due to torsional loading can be determined by rearranging Equation 56, which results in Equation 64:

$$\frac{\left(\frac{V}{V_p}\right)^2}{1-\frac{T}{T_p}}=1.0 \tag{64}$$

Combining Equations 63, 45 and 64 results in Equation 65.

$$\left(\frac{P_r}{P_y}\right)^2+\left(\frac{T_r}{T_p}\right)^2+\frac{\left(\frac{V_r}{V_p}\right)^4}{\left[1-\left(\frac{P_r}{P_y}\right)^2\right]\left(1-\frac{T_r}{T_p}\right)^2}+\left[\left(\frac{M_{rx}}{M_{px}}\right)^\alpha+\left(\frac{M_{rz}}{M_{pz}}\right)^\alpha\right]^{1/\alpha}\sqrt{1-\left(\frac{T_r}{T_p}\right)^2}=1.0 \tag{65}$$

where

M_{rx} = required x-axis bending moment, in.-kips
M_{rz} = required z-axis bending moment, in.-kips
P_r = required axial force, kips
T_r = required torsional moment, in.-kips
V_r = required shear force, kips

For biaxial shear, the transverse forces are combined vectorially, according to Equation 66:

$$V_r = \sqrt{V_{rx}^2 + V_{rz}^2} \tag{66}$$

where

V_{rx} = required x-axis shear force, in.-kips
V_{rz} = required z-axis shear force, in.-kips

Because the torsion strength can be greatly underestimated by neglecting the effects of warping and the Wagner effect, the detrimental effect of the second-order shear-torsion interaction term and the beneficial effect of the second-order moment-torsion interaction term can be neglected. Because the shear interaction term is conservative, based on the true limit load defined by Johnson et al. (1974), the second-order shear-axial interaction term can be neglected. Substituting a constant value of 1.7 for α and neglecting the second-order interaction terms for each independent load ratio results in Equation 67, which is proposed for design:

$$\left(\frac{P_r}{P_y}\right)^2 + \left(\frac{T_r}{T_p}\right)^2 + \left(\frac{V_r}{V_p}\right)^4 + \left[\left(\frac{M_{rx}}{M_{px}}\right)^{1.7} + \left(\frac{M_{rz}}{M_{pz}}\right)^{1.7}\right]^{0.59} = 1.0 \tag{67}$$

CONCLUSIONS

In design, many connection elements are modeled as rectangular members under various combinations of shear, flexural, torsional and axial loads. This paper shows that beam theory, and other design models using a first-yield criterion, severely underestimates the strength of rectangular connection elements. Existing research and new derivations were used to develop a plastic interaction equation, which has been proposed for design of rectangular elements subjected to any possible combination of loads. Experimental results are available for four load interaction cases: axial-flexure, shear-flexure, torsion-flexure and biaxial flexure. For these cases, the proposed interaction equation compares well with the experimental results. However, future testing may be needed to validate the equation for other load interaction cases.

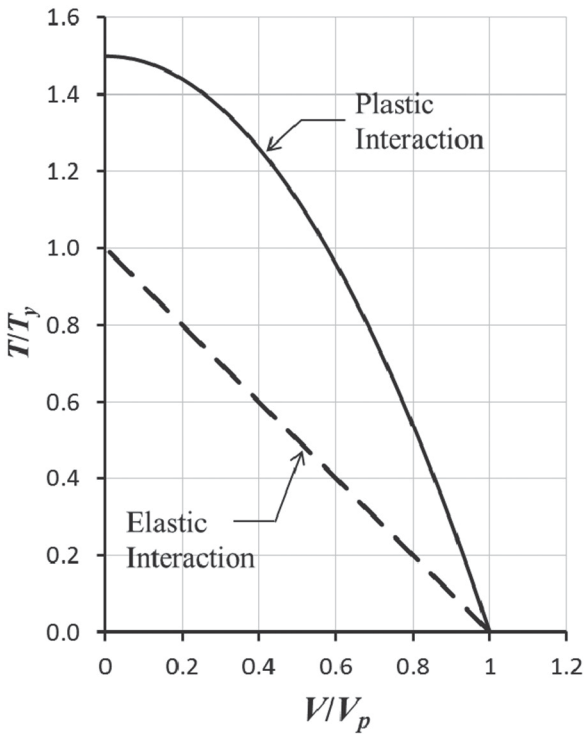

Fig. 13. Interaction of torsion and shear loads.

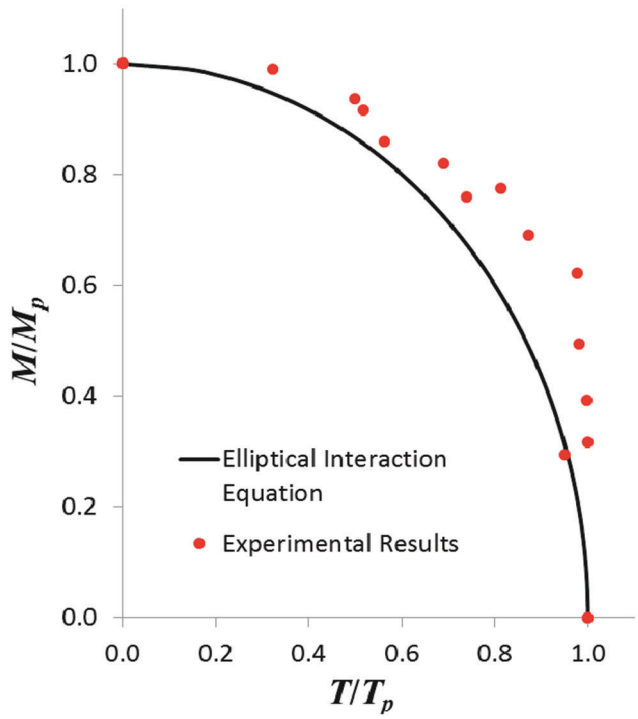

Fig. 14. Combined bending and torsion.

DESIGN EXAMPLE

In the vertical brace connection shown in Figure 15, the gusset yielding strength at the gusset-to-beam interface will be checked against the following loads, which were calculated with the uniform force method. The plate is ¾ in. thick and the material is ASTM A36.

LRFD	ASD
$H_b = 562$ kips $V_b = 64.0$ kips $M_b = 4{,}590$ kip-in.	$H_b = 375$ kips $V_b = 42.7$ kips $M_b = 3{,}060$ kip-in.

Because only shear, moment and axial loads are present, Equation 67 reduces to

$$\frac{M_r}{M_p}+\left(\frac{P_r}{P_y}\right)^2+\left(\frac{V_r}{V_p}\right)^4=1.0$$

For design, the interaction equations are

LRFD	ASD
$\frac{M_r}{\phi_b M_n}+\left(\frac{P_r}{\phi_t P_n}\right)^2+\left(\frac{V_r}{\phi_v V_n}\right)^4 \le 1.0$	$\frac{\Omega_b M_r}{M_n}+\left(\frac{\Omega_t P_r}{P_n}\right)^2+\left(\frac{\Omega_v V_r}{V_n}\right)^4 \le 1.0$

The flexural strength is calculated with AISC *Specification* Equation F11-1:

$$Z=\frac{(0.75\text{ in.})(47\text{ in.})^2}{4}$$
$$=414\text{ in.}^3$$

$$M_n = F_y Z$$
$$=(36\text{ ksi})(414\text{ in.}^3)$$
$$=14{,}900\text{ kip-in.}$$

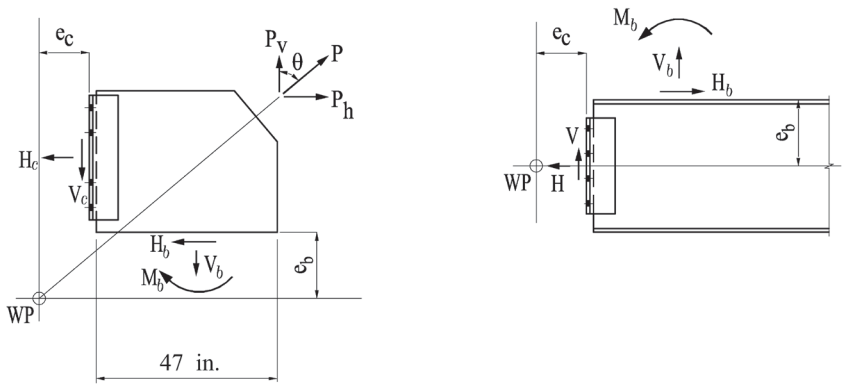

Fig. 15. Vertical brace connection.

LRFD	ASD
$\phi_t P_n = (0.9)(14{,}900 \text{ kip-in.})$ $= 13{,}400 \text{ kip-in.}$	$\frac{P_n}{\Omega_t} = \frac{14{,}900 \text{ kip-in.}}{1.67}$ $= 8{,}920 \text{ kip-in.}$

The tension yielding strength per AISC *Specification* Equation J4-1 is

$$P_n = F_y A_g$$
$$= (36 \text{ ksi})(0.75 \text{ in.})(47 \text{ in.})$$
$$= 1{,}270 \text{ kips}$$

LRFD	ASD
$\phi_t P_n = (0.9)(1{,}270 \text{ kips})$ $= 1{,}140 \text{ kips}$	$\frac{P_n}{t} = \frac{1{,}270 \text{ kips}}{1.67}$ $= 760 \text{ kips}$

The shear strength per AISC *Specification* Equation J4-3 is

$$V_n = 0.60 F_y A_{gv}$$
$$= (0.6)(36 \text{ ksi})(0.75 \text{ in.})(47 \text{ in.})$$
$$= 761 \text{ kips}$$

LRFD	ASD
$\phi_v V_n = (1.0)(761 \text{ kips})$ $= 761 \text{ kips}$	$\frac{V_n}{\Omega_v} = \frac{761 \text{ kips}}{1.50}$ $= 507 \text{ kips}$

Using the interaction equations,

LRFD	ASD
$\frac{4{,}590 \text{ kip-in.}}{13{,}400 \text{ kip-in.}} + \left(\frac{64.0 \text{ kips}}{1{,}140 \text{ kips}}\right)^2 + \left(\frac{562 \text{ kips}}{761 \text{ kips}}\right)^4$ $= 0.643 < 1.0$ **o.k.**	$\frac{3{,}060 \text{ kip-in.}}{8{,}920 \text{ kip-in.}} + \left(\frac{42.7 \text{ kips}}{760 \text{ kips}}\right)^2 + \left(\frac{375 \text{ kips}}{507 \text{ kips}}\right)^4$ $= 0.646 < 1.0$ **o.k.**

Therefore, the gusset-to-beam interface is adequate for the limit state of gusset plate yielding.

SYMBOLS

A = cross-sectional area, in.^{2}

F_y = specified minimum yield strength, ksi

G = shear modulus of elasticity = 11,200 ksi

I = moment of inertia, in.^{4}

J = torsional constant, in^4

L = length of the member, in.

M = bending moment, in.-kips

M_p = plastic bending moment, in.-kips

M_{px} = plastic bending moment about the x-axis, in.-kips

M_{pz} = plastic bending moment about the z-axis, in.-kips

M_{rx} = required x-axis bending moment, in.-kips

M_{rz} = required z-axis bending moment, in.-kips

M_x = bending moment about the x-axis, in.-kips

M_z = bending moment about the z-axis, in.-kips

P = axial force, kips

P_n = nominal axial strength, kips

P_r = required axial force, kips

Q = first moment of area, in.^{3}

S = gross section modulus, in.^{3}

T = torsional moment, in-kips

T_p = plastic torsional moment, in.-kips

T_r = required torsional moment, in.-kips

V = shear force, kips

V_r = required shear force, kips

V_{rx} = required x-axis shear force, in.-kips

V_{rz} = required z-axis shear force, in.-kips

a = plate dimension as shown in Figure 2a, in.

b = width of the central region of the cross-section resisting the shear force, in.

c = distance to outermost fiber, in.

d = depth of the member, in.

h = depth of the central region of the cross-section resisting the shear force, in.

h = depth of the central region of the cross-section resisting the axial force, in.

t = thickness of the member, in.

x = distance along the length of the member, in.

η = strain hardening modulus for pure shear

τ = shear stress, ksi

θ = angle of twist

θ = flexural rotation

θ_y = yield rotation

σ = normal stress, ksi

σ_e = effective stress, ksi

σ_x = normal stress in the x-direction, ksi

σ_y = tension yield stress, ksi

σ_z = normal stress in the z-direction, ksi

REFERENCES

AISC (2010), *Specification for Structural Steel Buildings*, American Institute of Steel Construction, Chicago, IL.

Ahmed, S.R., Idris, A.B.M. and Uddin, M.W. (1996), "Numerical Solution of Both Ends Fixed Deep Beams," *Computers and Structures*, Vol. 61, No. 1, pp. 21–29.

Astaneh, A. (1992), "Cyclic Behavior of Gusset Plate Connections in V-Braced Steel Frames," *Stability and Ductility of Steel Structures under Cyclic Loading*, Fukomoto, Y. and Lee, G. C., eds., CRC Press, Ann Arbor, MI, pp. 63–84.

Astaneh, A. (1998), "Seismic Behavior and Design of Gusset Plates," *Steel Tips*, Structural Steel Educational Council, December.

Balaz, I. and Kolekova, Y. (2002), "Warping," *Stability and Ductility of Steel Structures*, *Proceedings*, Otto Halasz Memorial Session, Ivanyi, M. and Akademiai Kiado, eds., Budapest.

Barry, J.E. and Ainso, H. (1983), "Single-Span Deep Beams," *Journal of Structural Engineering*, ASCE, Vol. 109, No. 3, pp. 646–663.

Billinghurst, A., Williams, J.R.L., Chen, G. and Trahair, N.S. (1992), "Inelastic Torsion of Steel Members," *Computers and Structures*, Vol. 42, No. 6, pp. 887–894.

Broude, B.M. (1953), *The Limit States of Steel Girders*, Moscow/Leningrad (in Russian).

Calladine, C.R. (1969), *Engineering Plasticity*, Pergamon Press, Oxford, United Kingdom.

Chakrabarty, J. (2006), *Theory of Plasticity*, 3rd ed., Elsevier.

Chen, W.F. and Atsuta, T. (1977), *Theory of Beam-Columns, Volume 2, Space Behavior and Design*, McGraw-Hill, New York, NY.

Chen, W.F. and Han, D.J. (2007), *Plasticity for Structural Engineers*, J. Ross Publishing, Plantation, FL.

Cook, R.D. and Young, W.C. (1985), *Advanced Mechanics of Materials*, Macmillan Publishing Company, New York, NY.

Drucker, D.C. (1956), "The Effect of Shear on the Plastic Bending of Beams," *Journal of Applied Mechanics*, December, pp. 509–514.

Duan, L. and Chen, W.F. (1989), "Design Interaction Equation for Steel Beam-Columns," *Journal of Structural Engineering*, ASCE, Vol. 115, No. 5, pp. 1225–1243.

Freudenthal, A.M. (1950), *The Inelastic Behavior of Engineering Materials and Structures*, John Wiley and Sons, New York, NY.

Galambos, T.V. and Surovek, A.E. (2008), *Structural Stability of Steel*, John Wiley and Sons, New York, NY.

Gill, S.S. and Boucher, J.K.G. (1964), "An Experimental Investigation of Plastic Collapse of Structural Members under Combined Bending and Torsion," *The Structural Engineer*, Vol. 42, No. 12, pp. 423–428.

Goodrich, W. (2005), *Behavior of Extended Shear Tabs in Stiffened Beam-to-Column Connections*, Master's Thesis, Vanderbilt University.

Gregory, M. (1960), "The Bending and Shortening Effect of Pure Torque," *Australian Journal of Applied Science*, March, pp. 209–216.

Hardin, B.O. (1958), "Experimental Investigation of the Primary Stress Distribution in the Gusset Plates of a Double Plane Pratt Truss Joint with Chord Splice at the Joint," University of Kentucky Engineering Experiment Station, Bulletin No. 49, September.

Harrison, H.B. (1963), "The Plastic Behavior of Mild Steel Beams of Rectangular Section Bent About Both Principal Axes," *The Structural Engineer*, Vol. 41, No. 7, pp. 231–237.

Hill, R. and Siebel, M.P.L. (1953), "On the Plastic Distortion of Solid Bars by Combined Bending and Twisting," *Journal of the Mechanics and Physics of Solids*, Vol. 1, pp. 207–214.

Horne, M.R. (1951), "The Plastic Theory of Bending of Mild Steel Beams with Particular Reference to the Effect of Shear Forces," *Proceedings of the Royal Society of London, Series A, Mathematical and Physical Sciences*, Vol. 207, No. 1089, pp. 216–228.

Irvan, W.G. (1957), "Experimental Study of Primary Stresses in Gusset Plates of a Double Plane Pratt Truss," University of Kentucky Engineering Research Station, Bulletin No. 46, December.

Jensen, C.D. and Crispen, R.E. (1938), "Stress Distribution in Welds Subject to Bending," *Welding Research Supplement*, American Welding Society, October.

Johnson, W., Chitkara, N.R. and Ranshi, A.S. (1974), "Plane-Stress Yielding of Cantilevers in Bending Due to Combined Shear and Axial Load," *Journal of Strain Analysis*, Vol. 9, No. 2, pp. 67–77.

Karr, P.H. (1956), "Stresses in Centrally Loaded Deep Beams," *SESA Proceedings*, Vol. XV, No. 1, Society for Experimental Stress Analysis, pp. 77–84.

Lavis, C.S. (1967), *Computer Analysis of the Stresses in a Gusset Plate*, Master's Thesis, University of Washington.

May, I.M. and Al-Shaarbaf, I.A.S. (1989), "Elasto-Plastic Analysis of Torsion Using a Three-Dimensional Finite Element Model," *Computers and Structures*, Vol. 33, No. 3, pp. 667-678.

Metzger, K.A.B. (2006), "Experimental Verification of a New Single Plate Shear Connection Design Model," Master's Thesis, Virginia Polytechnic Institute, May 4.

Mohr, B.A. and Murray, T.M. (2008), "Bending Strength of Steel Bracket and Splice Plates," *Engineering Journal*, AISC, Vol. 45, No. 2, pp. 97–106.

Moore, D.B. and Owens, G.W. (1992), "Verification of Design Methods for Finplate Connections," *The Structural Engineer,* Vol. 70, No. 3/4, February.

Morris, G.A. and Fenves, S.J. (1969), "Approximate Yield Surface Equations," *Journal of the Engineering Mechanics Division*, ASCE, Vol. 95, No. EM4, pp. 937–954.

Mrazik, A., Skaloud, M. and Tochacek, M. (1987), *Plastic Design of Steel Structures*, Ellis Horwood Series, Engineering Science, Halsted Press, New York, NY.

Nadai, A. (1950), *Theory of Flow and Fracture of Solids*, McGraw-Hill, New York, NY.

Neal, B. G. (1961), "The Effect of Shear and Normal Forces on the Fully Plastic Moment of a Beam of Rectangular Cross Section," *Journal of Applied Mechanics*, Vol. 28, pp. 269–274.

Neal, B.G. (1963), *The Plastic Methods of Structural Analysis*, 2nd ed., John Wiley and Sons, New York, NY.

Ocel, J.M. (2013), "Guidelines for the Load and Resistance Factor Design and Rating of Riveted and Bolted Gusset-Plate Connections for Steel Bridges," Contractor's Final Report for NCHRP Project 12-84, National Cooperative Highway Research Program, February.

Paltchevskiy, S.A. (1948), *Determination of Load-Carrying Capacity of Steel Bars for Some Cases of Complex State of Stress* (in Russian).

Patrick, M., Thomas, I.R. and Bennets, I.D. (1986), "Testing of Web Side Plate Connection," *Proceedings of the Pacific Structural Steel Conference*, Vol. 2, New Zealand Heavy Engineering Research Association, pp. 95–116.

Perna, F.J. (1941), "Photoelastic Stress Analysis, with Special Reference to Stresses in Gusset Plates," Master's Thesis, University of Tennessee.

Rust, T.H. (1938), "Specification and Design of Steel Gussett-Plates," *Proceedings,* ASCE, November, pp. 142–167.

Sanatthadaporn, S. and Chen, W.F. (1970), "Interaction Curves for Sections Under Combined Biaxial Bending and Axial Force," WRC Bulletin No. 148, Welding Research Council, New York, pp. 1–11.

Sandel, J.A. (1950), *Photoelastic Analysis of Gusset Plates*, Masters Thesis, University of Tennessee, December.

Schreiner, N.G. (1935), "Behavior of Fillet Welds When Subjected to Bending Stresses," *Welding Journal*, American Welding Society, September.

Seaburg, P.A. and Carter, C.J. (1997), *Torsional Analysis of Structural Steel Members*, Design Guide 9, American Institute of Steel Construction, Chicago, IL.

Seely, F.B. and Putnam, W.K. (1919), "The Relation Between the Elastic Strengths of Steel in Tension, Compression and Shear," Bulletin No. 115, Engineering Experiment Station, Vol. 17, No. 11, University of Illinois, November 10.

Seely, F.B. and Smith, J.O. (1952), *Advanced Mechanics of Materials*, John Wiley and Sons, New York, NY.

Shawki, S. and Hendry, A.W. (1961), "Stresses in a Deep Beam with a Central Concentrated Load," *Experimental Mechanics*, June, pp. 192–198.

Sheridan, M.L. (1953), "An Experimental Study of the Stress and Strain Distribution in Steel Gusset Plates," Ph.D. Dissertation, University of Michigan, Ann Arbor, MI.

Sherman, D.R. and Ghorbanpoor, A. (2002), "Design of Extended Shear Tabs," Final Report, American Institute of Steel Construction, Chicago, IL, October.

Shunsuke, B. and Kajita, T. (1982), "Plastic Analysis of Torsion of a Prismatic Beam," *International Journal for Numerical Methods in Engineering*, Vol. 18, pp. 927–944.

Sidebottom, O.M. and Clark, M.E. (1958), "Theoretical and Experimental Analysis of Members Loaded Eccentrically and Inelastically," Engineering Experiment Station, Bulletin No. 447, University of Illinois, March.

Smith, J.O. and Sidebottom, O.M. (1965), *Inelastic Behavior of Load-Carrying Members*, John Wiley and Sons, New York, NY.

Steele, M.C. (1954), "The Plastic Bending and Twisting of Square Section Members," *Journal of the Mechanics and Physics of Solids*, Vol. 3, pp. 156–166.

Struik, J.H.A. (1972), "Applications of Finite Element Analysis to Non-linear Plane Stress Problems, Ph.D. Dissertation, Lehigh University.

Vasarhelyi, D.D. (1971), "Tests of Gusset Plate Models." *Journal of the Structural Division,* ASCE Vol. 97, No. fST2, pp. 665–679.

Vrouwenvelder, A.C.W.M. (2003), *The Plastic Behavior and the Calculation of Beams and Frames Subjected to Bending*, Technical University Delft, March.

White, D.W., Leon, R.T., Kim, Y.D., Mentes, Y. and Bhuiyan, M.T.R. (2013), "Finite Element Simulation and Assessment of the Strength Behavior of Rivited and Bolted Gusset-Plate Connections in Steel Truss Bridges," Final Report Prepared for Federal Highway Administration and NCHRP Transportation Research Board of the National Academies, March.

Whitmore, R.E. (1952), "Experimental Investigation of Stresses in Gusset Plates," University of Tennessee Engineering Experiment Station, Bulletin No. 16, May.

Wyss, T. (1923), "Die Kraftfelder in Festen Elastischen Korpern und ihre Praktischen Anwendungen," Berlin, Germany.